MAGMA (2004) 16: 174–181
DOI 10.1007/s10334-003-0025-5

RESEARCH ARTICLE

Beathe Sitter
Tone Bathen
Bjørn Hagen
Cecilie Arentz
Finn Egil Skjeldestad
Ingrid S. Gribbestad

Cervical cancer tissue characterized by high-resolution magic angle spinning MR spectroscopy

Received: 27 June 2003
Accepted: 3 November 2003
Published online: 27 February 2004

B. Sitter (✉) · T. Bathen
I. S. Gribbestad
SINTEF Unimed,
7465 Trondheim, Norway
E-mail: beathe.sitter@medisin.ntnu.no

B. Sitter
Department of Neuroscience,
Faculty of Medicine,
Norwegian University of Science
and Technology (NTNU)

B. Hagen · F. E. Skjeldestad
Institute of Laboratory Medicine,
Children and Woman's Diseases,
Norwegian University of Science
and Technology (NTNU)

C. Arentz
Department of Physics,
Norwegian University of Science
and Technology (NTNU)

F. E. Skjeldestad
Section of epidemiological research,
Unimed, SINTEF

I. S. Gribbestad
Clinical Cancer Research Unit,
Cancer Clinic, St. Olav University Hospital,
7465 Trondheim, Norway

Abstract *Objective*: In recent years, high-resolution magic angle spinning (HR MAS) has provided the opportunity to explore detailed biochemical composition of intact tissue. Previous studies of intact cervical biopsies with high-resolution magnetic resonance spectroscopy (MRS) have correlated well with histopathology. Lactate level in cervical cancer tissue has been found to correlate to metastatic spread. The purpose of this study was to explore the potential of the HR MAS technique as a tool for chemical characterization of cervical cancer tissue. *Materials and methods*: Tissue samples from the cervix were collected after hysterectomy from patients with cervical cancer ($n = 8$) and patients with nonmalignant disease ($n = 8$). The tissue specimens were analyzed using HR MAS MR spectroscopy combined with principal component analysis (PCA). *Results*: The resulting spectra showed resolution comparable with high-resolution MR spectra of extracts. Multivariate analysis confirmed that MAS spectra classified according to patient diagnosis. *Conclusion*: Malignant tissue of the cervix differed from nonmalignant tissue with regard to higher levels of cholines and amino acid residues and lower levels of glucose.

Keywords Cervical cancer · MR spectroscopy · Choline · Principal component analysis

Abbreviations *Cho* choline · *GPC* glycerophosphocholine · *MAS* magic angle spinning · *PC* phosphocholine · *PCA* principal component analysis

Introduction

Cervical cancer represents nearly 10% of all cancers in women from the western world [1]. Screening programs in developed countries have contributed to a decline in incidence and mortality over the last 50 years; in less developed countries, however, screening has often not been established and cervical cancer is the most frequent cancer form in women in many third world countries [2].

Tissue from cervical cancer patients have been examined by magnetic resonance (MR) spectroscopy (MRS) in vivo [3, 4], and Lee et al. [3] found that spectra of adenocarcinomas differed slightly from those from squamous cell carcinomas. Furthermore, Mountford et al. have shown that standard proton MRS of tissue

samples can distinguish inflammation from malignant lesions in the cervix [5]. In a later work [6], the same research group was able to separate invasive and preinvasive lesions applying proton MRS. The results from these studies, which are based on broad and overlapping resonances, indicate that higher resolved spectra can provide more detailed information in cervical cancer tissue.

Progress has been made in in vitro MR analysis of tissue samples due to the implementation of high-resolution magic angle spinning (HR MAS) spectroscopy. In tissue, restriction of molecular motion and magnetic susceptibility results in spectral broadening as compared with liquids. Rapidly spinning the sample around its own axis in a 54.7° angle to the static magnetic field, the so-called magic angle, eliminates some of the factors contributing to line broadening. The result is spectra of intact tissue samples with resolution comparable with high-resolution spectra of extracts [7]. MAS spectroscopy has been applied in various studies of human tissues and diseases, such as cancers of the brain [8], prostate [9], and breast [10].

Because MRS allows identification of a large number of metabolites simultaneously, the vast amount of information makes visual inspection and analysis difficult. Spectra of tumors are often found to differ from spectra of nonmalignant tissue in intensities of almost all peaks [11, 12], and multivariate analysis of the full MR spectra has proven useful in interpreting the MR findings [13, 14].

The purpose of this study was to evaluate HR MAS analysis of tissue from the uterine cervix as a tool in cancer metabolic studies. MR spectra were obtained from biopsy material from the cervix from patients with cervical cancer and compared with spectra from cervical biopsies from patients without cancer. Multivariate analysis of the HR MAS spectra was used to evaluate whether classification of the different tissue types was in accordance with patient diagnosis. The MR spectra were explored in detail in an attempt to reveal the biochemical composition of the tissues and identify characteristics of tumor tissue.

Methods

Subjects

Eight women with a mean age of 50 years (range 39–67), who underwent hysterectomy due to cervical cancer, were included in the study. None of the patients received any anticancer treatment prior to hysterectomy. Histopathological examination of the surgical specimens revealed six squamous cell carcinomas (stages IB and IIA) and two adenocarcinomas (stage IIB). Two of the patients with squamous cell carcinomas had lymphatic spread. In addition, eight women, mean age 50 years (range 29–69), who underwent hysterectomy for various benign reasons, served as controls.

Samples

After excision, the uterus was kept in saline compresses until tissue specimens were taken from the cervix uteri as soon as possible after surgery. The sample for MAS was taken from a tumor-representative site in the fresh surgical specimen. A total of 16 samples was obtained. The samples were stored in liquid nitrogen until HR MAS MR spectroscopic analysis. Samples were cut to fit a 4-mm (o.d.) rotor and added D_2O before MR analysis.

MR experiments

High-resolution proton MAS spectra were recorded using a BRUKER AVANCE DRX600 spectrometer equipped with a $^{1}H/^{13}C$ MAS probe with possibilities for a gradient along the magic angle axis (BRUKER Analytic, Germany). Samples were spun at 6 kHz and acquisitions obtained using two different one-dimensional sequences for each sample. Water-suppressed spectra were acquired using a single pulse sequence with 2 seconds preirradiation of the water resonance (zgpr, BRUKER) before a 60-degree pulse angle was applied. The second type of spectra was acquired using a spin-echo sequence with water suppression (2 seconds) included (cpmgpr, BRUKER). The acquisitions were performed with a delay of 1 ms repeated 136 times, giving spectra with a total echo time of 285 ms. For both experiments, 128 transients over a spectral region of 10 kHz were collected into 32K points, giving an acquisition time of 1.64 seconds. All experiments were performed at room temperature. The raw data were multiplied with 0.7 Hz exponential line broadening before Fourier transformation into 64K points. Chemical shift referencing was done relative to the methyl group in the lactate resonance, which shifts 1.32 ppm downfield from TSP.

J-resolved spectra were obtained by a standard spin-echo sequence with 2 s water presaturation (Jrespr, BRUKER). Eight transients were collected into 8K data points of 10 kHz spectral region. The interpulse delay was incremented 64 times with 6.4 ms, resulting in 78.1 Hz spectral region in the F1 dimension. The raw data were processed using a sine window function in both dimensions, tilted and symmetrized. Homonuclear correlated spectra (COSY; cosygspr, BRUKER) were recorded by acquisition of 16 transients per increment for 512 increments collected into 2K data points. A spectral width of 8 kHz was used in both dimensions. The time domain data were zero filled and multiplied with a sine window function in both dimensions before Fourier transform.

Multivariate analysis

Water-suppressed and spin-echo spectra were used as inputs in two separate PC analyses.

Water suppressed spectra were Fourier transformed after applying 0.7 Hz exponential line broadening. Baseline offset was adjusted and chemical shifts were referenced to the lactate doublet (1.32 ppm). The spectral regions 0.0–4.5 ppm were saved and collected into one matrix of 16 samples × 2,945 variables.

The FIDs from spin-echo acquisitions were Fourier transformed without window function. Baseline offset was adjusted and chemical shifts were referenced to the lactate doublet (1.32 ppm). The regions from 1.4 to 4.3 ppm were saved as ASCII files and collected into a matrix of 16 samples × 2,700 variables.

For both matrices, the spectra were normalized to the area below the curve (mean normalization). Principal component analysis (PCA) was carried out in an unsupervised manner and was performed with full cross-validation and mean centering [15]. The score plots were examined for correlation with patient diagnosis and age, and the time period samples were subject to room temperature before spectral recordings.

Results

HR MAS ^{1}H spin-echo spectra of biopsies from cervix gave good signal resolution, allowing almost complete separation of the different compounds in the one-dimensional spectra. Additional information from two-dimensional spectra and literature values [7, 16, 17] enabled almost total spectral assignment, providing detailed information on the biological composition of the different tissue samples. In Fig. 1, a ^{1}H spin-echo HR MAS spectrum of cervical tissue specimens from a patient with cervical cancer is shown. The assignments in the figure correspond with the data in Table 1.

Representative spin-echo MAS spectra of cervix uteri tissue specimens from one cervix cancer patient and one control patient are presented in Fig. 2. All spectra showed high resolution. The vast majority of peaks were of similar intensity in all spectra and visual inspection between the two groups revealed very few differences. Spin-echo recorded MAS spectra of the malignant cervical samples deviated from spectra of nonmalignant tissues in levels of glucose and uracil. Glucose was detected in all but one of the eight nonmalignant tissue specimens, but in only three of the eight cervix cancer tissue specimens. Uracil was found in all cervical cancer samples, but could not be detected in any of the nonmalignant tissue specimens. Furthermore, an unas-

Fig. 1 High-resolution spin-echo proton MAS spectra of cervix cancer biopsy from patient diagnosed with squamous cell carcinoma of the cervix uterus. Assignments are given in Table 1. Scaling of the three different parts of the spectrum is done individually and led to cutting the lactate doublet at 1.33 ppm. The spectral region from 5.5 to 4.7 ppm has been excluded. For detailed acquisition parameters, see "Methods"

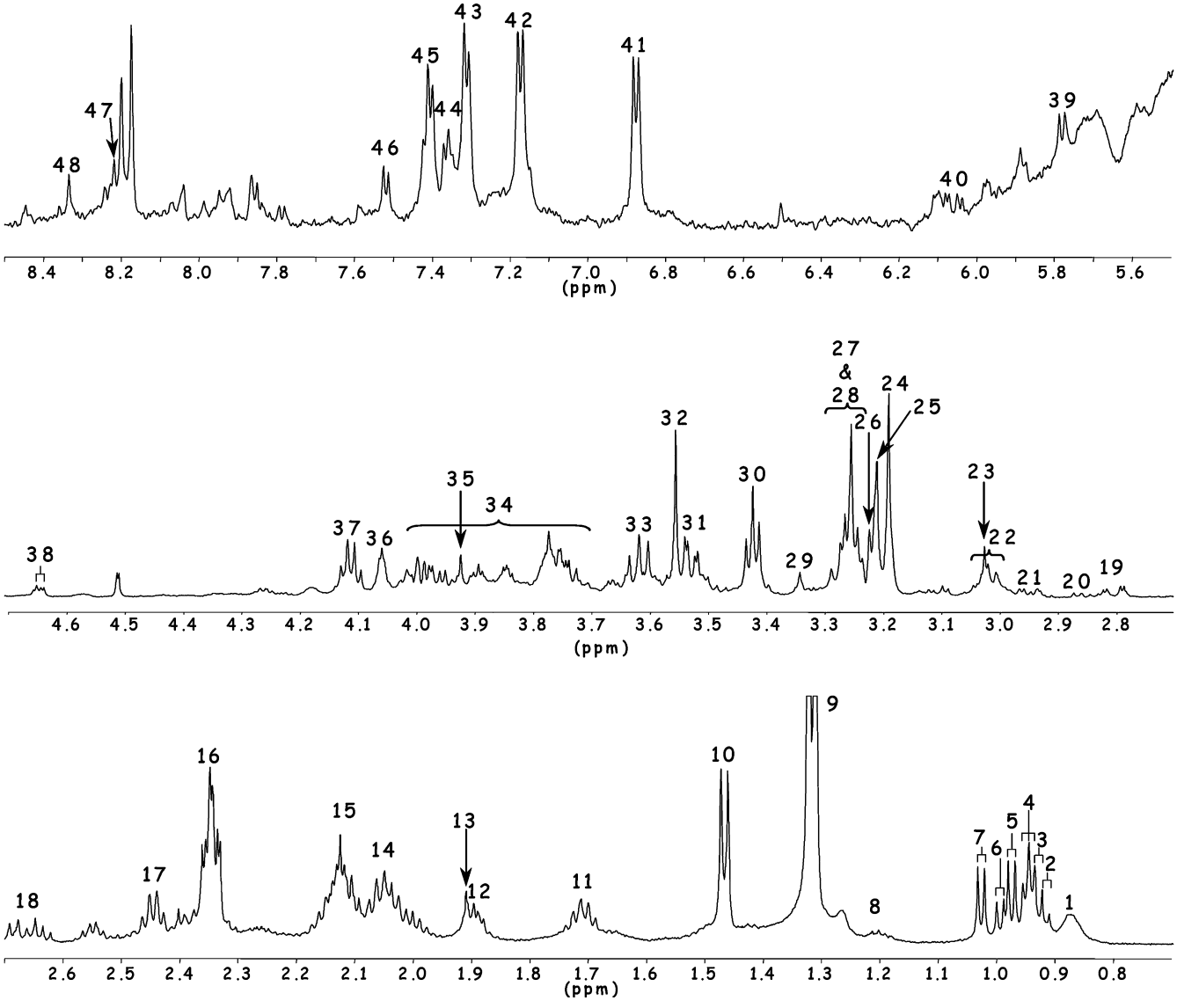

signed peak was detected at 2.02 ppm in the spectrum from one of the two adenocarcinomas, shown in Fig. 2A.

The water-suppressed spectra were used to calculate fatty acid CH_2/CH_3 ratio based on the intensity of the broad resonances at 1.3 and 0.9 ppm respectively (spectra not shown). Cervical cancer samples showed a slightly higher ratio (1.57 ± 0.20) than nonmalignant cervical samples (1.50 ± 0.20), but the difference was not significant.

Table 1 Tentative ^{1}H chemical shift assignment on HR MAS spectra of cervical and uterine tissue samples. Assigned numbers correspond to numbering in Fig. 1

Metabolite		Assigned number	^{1}H Multipl.	chem. shift (ppm)
Fatty acids	$-CH_3$	1	t	0.87
Isoleucine	δCH_3	2	t	0.93
Leucine	$\delta' CH_3$	3	d	0.94
Leucine	δCH_3	4	d	0.96
Valine	γCH_3	5	d	0.98
Isoleucine	γCH_3	6	d	1.00
Valine	$\gamma' CH_3$	7	d	1.03
β-hydroxybutyrate	CH_3	8	d	1.19
Lactate	CH_3	9	d	1.32
Alanine	CH_3	10	d	1.47
Lysine	δCH_2	11	m	1.72
Lysine	βCH_2	12	m	1.90
Acetate	(CH_3)	13	s	1.91
Glutamate	βCH_2	14	c	2.05
Glutamine	βCH_2	15	c	2.13
Glutamate	γCH_2	16	dt	2.34
Glutamine	γCH_2	17	c	2.45
Aspartate	βCH	18	dd	2.67
Aspartate	$\beta' CH$	19	dd	2.80
Aspargine	βCH	20	dd	2.87
Aspargine	$\beta' CH$	21	dd	2.95
Lysine	εCH_2	22	t	3.02
Creatine	CH_3	23	s	3.03
Choline	$N(CH_3)_3$	24	s	3.19
Glycerophospho-choline	$N(CH_3)_3$	25	s	3.21
Phosphocholine	$N(CH_3)_3$	26	s	3.21
Taurine	$N\text{-}CH_2$	27	t	3.25
myo-Inositol	C5H	28	t	3.27
scyllo-Inositol		29	s	3.34
Taurine	$S\text{-}CH_2$	30	t	3.42
myo-Inositol	C1H, C3H	31	dd	3.53
Glycine	αCH_2	32	s	3.55
myo-Inositol	C4H, C6H	33	dd	3.61
Amino acid residues	αCH	34		3.75–4.00
Creatine	CH_2	35	s	3.92
myo-Inositol	C2H	36	t	4.05
Lactate	CH	37	q	4.11
β-Glucose	C1H	38	d	4.64
Uracil	C6H, ring	39	d	5.79
Inosine	C1H ribose	40	d	5.88
Tyrosine	C3H, 5H ring	41	d	5.88
Tyrosine	C2H, 6H ring	42	d	7.18
Phenylalanine	C2H, C6H, ring	43	m	7.32
Phenylalanine	C4H, ring	44	m	7.36
Phenylalanine	C3H, C5H, ring	45	m	7.41
Uracil	C5H, ring	46	d	7.86
Inosine	C2, ring	47	s	8.22
Inosine	C8, ring	48	s	8.34

The results from the multivariate analysis of the MR spectra are presented in Figs 3 and 4. Both principal component analyses showed that the MAS spectra describe biochemical properties that discriminate between malignant and nonmalignant cervical tissue. Sample score values did not correlate with patient age or the time period samples were subject to room temperature.

In Fig. 3A, the score plot of principal components 1 and 2 from PCA of Water-suppressed spectra from cervical tissue are presented. The malignant samples (X) can be separated from the nonmalignant samples (O) by a linear decision boundary. Tissue from cervical cancer patients mainly differed from tissue from controls in high score for the first principal component (PC1). The four cancer samples showing the highest scores for PC1 are the two adenocarcinomas (X_A) and the biopsies from the two patients with lymphatic spread (X_L). This principal component (Fig. 3B), describing 63% of the variation in the spectra, is dominated by lactate, the methyl and methylene groups of lipids, and to some extent, choline-containing compounds. The higher scores for PC1 of cervical cancer samples imply that they have higher contents of these compounds than the nonmalignant cervical samples.

Figure 4A gives the score plot of the first two principal components from PCA of the spin-echo recorded spectra and describes 57% of the total variation in the original 16 spectra. Spectra of cervical cancer biopsies (X) and noninvolved cervical tissue (O) are situated in two distinct groups that can be separated based on their different scores for PC1. Examination of the loading profile of PC1 (Fig. 4B) shows that the samples from patients with cervical cancer may be associated with higher concentrations of cholines (Cho, PC, GPC) and amino acid residues (creatine, taurine, and alanine). In addition, the cancer samples seem to have reduced levels of glucose.

Discussion

Previous reports on MR spectroscopy of cervical cancer biopsies have largely been concerned with lipids and lipid ratios [6, 18]. The CH_2/CH_3 ratio we found for the malignant lesions (1.57) was lower than the ratio (1.89) reported by Delikatny et al. [6], whereas our finding for the noninvolved specimens was higher (1.50/1.28).

Principal component analysis was found to be a better approach for analyzing the HR MAS spectra of cervical specimens. Analysis of the water-suppressed

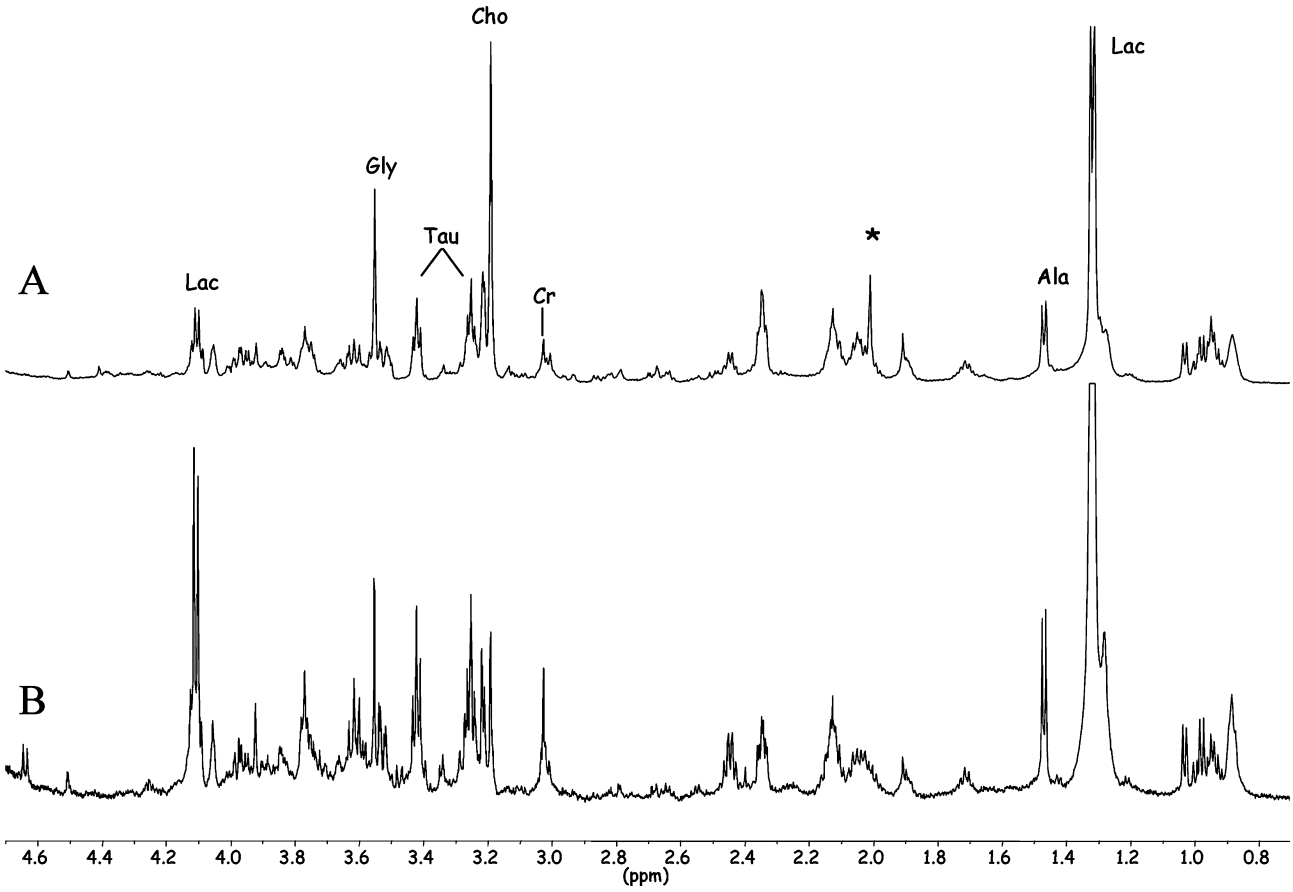

Fig. 2 Spin-echo proton MAS spectra of biopsy samples from (**A**) cervix uterus from cervical cancer patient diagnosed with adenocarcinoma and (**B**) cervix uterus from control. Scaling of the spectra led to cutting of the lactate doublet at 1.33 ppm. For full spectral assignments, see Fig. 1. Abbreviations used in annotations: Lac, lactate; Gly, glycine; Tau, taurine; Cho, choline; Cr, creatine; and Ala, alanine. The peak labeled * is unassigned. For detailed acquisition parameters, see "Methods"

spectra, dominated by lipid signals, led to discrimination of adenocarcinomas and squamous cell carcinomas with lymphatic spread. The spin-echo spectra, where contributions from lipids and other broad resonances are suppressed, separated malignant cervical tissue from noninvolved. The region on the low-field side of the water peak was omitted from the spectra in both multivariate analyses because peaks in this area have intensity variations due to water saturation. Furthermore, the lactate peak at 1.32 ppm was excluded for PCA of spin-echo spectra because the remaining lipid signals influence the intensity of the lactate peak.

The HR MAS spectra of cervix cancer tissue and nonmalignant cervix tissue are dominated by the same metabolites. Classification of the tissue types is made on relative amounts of the same metabolites. As can be seen in the loading profile of PC1 in Fig. 4B, the metabolites that contribute most to classification of the spectra are present in high amounts in all samples.

The loading profile in Fig. 4B shows that lowered glucose levels contribute to the characterization of cervical cancer tissue. This correlates with undetectable levels of glucose in five out of eight MAS spectra of malignant samples. Decreased glucose levels in tumor tissue is due to elevated energy requirement in the proliferation process, and numerous studies have been performed on the increased glucose metabolism in tumors [19, 20] since the Warburg effect was first presented in 1930 [21].

Furthermore, PCA of spin-echo MAS spectra shows that there is extensive variation in creatine concentration among the samples. This indicates the inaccuracy that may occur when utilizing creatine as an internal concentration standard.

The relative concentrations of all cholines were found to be higher in the cervical cancer biopsies. GPC, PC and Cho are important metabolites in the phospholipid metabolism and are thus believed to play roles as tumor markers, describing an increased cell turnover. In vivo MRS has been shown to differentiate between malignant and benign breast lesions based on the choline compounds [22]. The relative concentration of taurine was

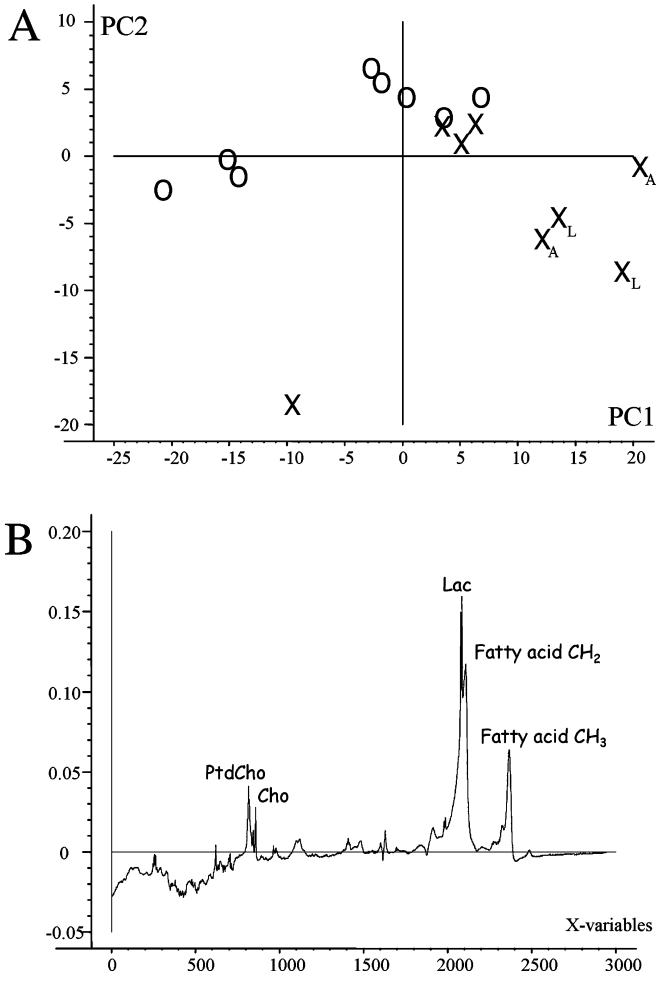

Fig. 3 Score plot of PC1 and PC2 from principal component analysis of the spectral region 0–4.5 ppm of the water-suppressed MAS spectra of biopsies from the cervix from 16 patients. PC1 and PC2 account for 80% of the variation in the spectra. O denotes cervix tissue from noncancer patients while X denotes cervical cancer tissue. The adenocarcinomas and cervical cancer samples from patients with lymphatic spread were denoted X_A and X_L respectively. **B** Loading profile of PC1, representing 63% of the spectral variations. Abbreviations used in assignments: PtdCho, phosphatidylcholine; Cho, choline; and Lac, lactate

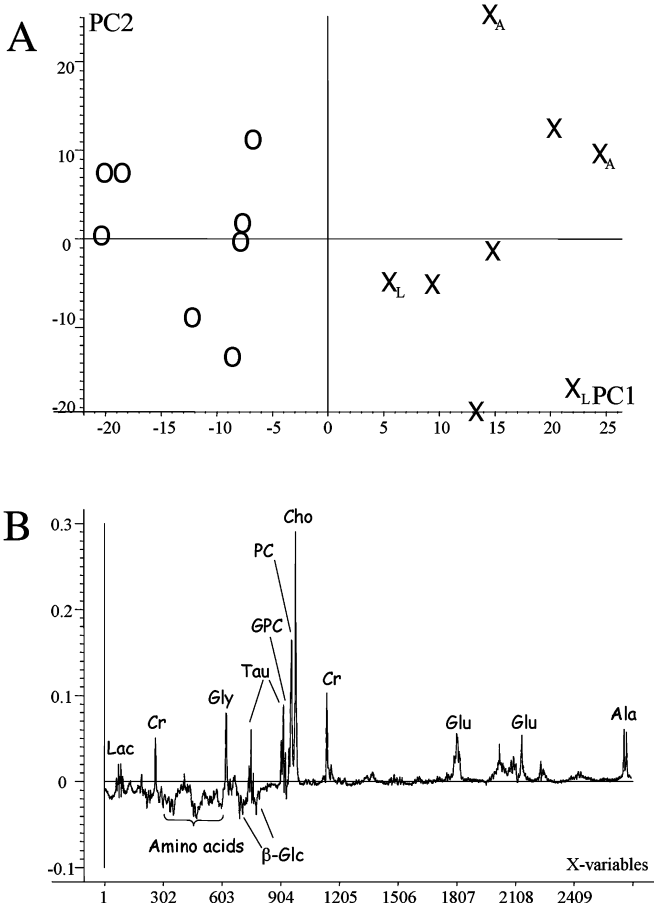

Fig. 4 **A** Score plot of PC1 and PC2 from principal component analysis of the spectral region 4.1–1.4 ppm from spin-echo MAS spectra of biopsies from cervix from 16 patients. PC1 and PC2 account for 55% of the variation in the spectra. X denotes cervical cancer tissue, while O denotes cervix tissue from non-cancer patients. The adenocarcinomas and cervical cancer samples from patients with lymphatic spread were denoted X_A and X_L respectively. **B** Loading profile of PC1. Abbreviations used in assignments: Cr, creatine; Gly, glycine; Tau, taurine; β-Glc, β-glucose; GPC, glycerophosphocholine; PC, phosphocholine; Cho, choline; Glu, glutamate; and Ala, alanine

found to be higher in cervical cancer tissue than in the cervical control tissue. Taurine has been shown to be present in high levels in breast cancerous tissue [23, 24]. It is possible that this rise in taurine levels may be an endogenous defense mechanism against tumor proliferation. Relative levels of glycine were also found to be higher in cervical cancer biopsies. In a study concerning in vitro MRS on specimens of human brain tumors, gliomas were characterized by an increase of the ratios of alanine, choline and glycine over creatine [25].

The peak detected at 2.02 ppm in the spectrum from one of the two adenocarcinomas is probably the same peak as previously reported in six out of seven adenocarcinomas studied by in vivo MRS by Lee et al. [3]. Further two-dimensional spectroscopic analysis of tissue samples should be performed to assign this peak in HR MAS MR spectra.

Walenta et al. [26] found that lactate levels correlated with metastatic spread. Lactate was found to contribute in discriminating adenocarcinomas and samples from patients with lymphatic spread (Fig. 3). The methyl and methylene peaks from lipids contribute to this discrimination, which imply a relatively higher content of lipids. Altered lipid profiles in malignant tissue has been reported in several studies [18, 27, 28].

The tissue biopsies were analyzed at room temperature. Sample temperatures were calculated to 26.17 °C

(range 25.1–27.5 °C) from the 10 spin-echo spectra where glucose was detectable [29]. Samples have been exposed to room temperature for 1.6 hours on average prior to the MR acquisition. Biochemical degradation is assumed to be distinctive. Because lactate is a product of anaerobic degradation of glucose, classification influenced by these metabolites can be unreliable.

The MR spectra enabled classification, even though degradation of metabolites had occurred. Because no clear correlation was found between sample score (Figs 3A and 4A) and time period, metabolic degradation was assumed to be similar at room temperature for the two tissue types. This implies that some of the observed spectral features have to be tissue dependent. Spin-echo spectra, containing signals from small, water-soluble molecules, separate malignant from non-malignant cervical tissue. This result implies that the spectra from malignant samples contain metabolic information specific for cancerous tissue. Spectra including lipids and macromolecules might contain metabolic information that can distinguish types of cervical cancers and maybe predict metastasis. The experimental conditions, however, require caution in interpreting metabolic differences. Further investigations should be performed at low temperature (4 °C) to reduce metabolic degradation and on samples of cytological size.

Combined with multivariate analysis, MR spectra of intact tissue biopsies from cervix uteri discriminate between cancerous and normal cervical tissue. In addition, the high resolution of the HR MAS spectra of tissue specimens from the cervix provides detailed information on the biochemical composition of the tissues. Studies of samples from a larger number of patients are needed in order to evaluate the clinical value of this method in the pathology of cervix uteri.

References

1. Franco EL, Duarte-Franco E, Ferenczy A (2001) Cervical cancer: epidemiology, prevention and the role of human papillomavirus infection. Can Med Assoc J 164:1017–1025
2. Kleihues P, Stewart BW, World Health Organization. (2003) World cancer report. WHO, IARC Press, Lyon
3. Lee JH, Cho KS, Kim Y-M et al (1998) Localized in vivo ^{1}H nuclear MR spectroscopy for evaluation of human uterine cervical carcinoma. Am J Roentgenol 170:1279–1282
4. Allen JR, Prost RW, Griffith OW et al (2001) In vivo proton (H1) magnetic resonance spectroscopy for cervical carcinoma. Am J Clin Oncol 24:522–529
5. Mountford CE, Delikatny EJ, Dyne M et al (1990) Uterine cervical punch biopsy specimens can be analyzed by ^{1}H MRS. Magn Reson Med 13:324–331
6. Delikatny EJ, Russell P, Hunter JC et al (1993) Proton MR and human cervical neoplasia: ex vivo spectroscopy allows distinction of invasive carcinoma of the cervix from carcinoma in situ and other preinvasive lesions. Radiology 188:791–796
7. Sitter B, Sonnewald U, Spraul M et al (2002) High-resolution magic angle spinning MRS of breast cancer tissue. NMR Biomed 15:327–337
8. Cheng LL, Chang I-W, Louis DN et al (1998) Correlation of high-resolution magic angle spinning proton magnetic resonance spectroscopy with histopathology of intact human brain tumor specimens. Cancer Res 58:1825–1832
9. Kurhanewicz J, Swanson MG, Nelson SJ et al (2002) Combined magnetic resonance imaging and spectroscopic imaging approach to molecular imaging of prostate cancer. J Magn Reson Imaging 16:451–463
10. Cheng LL, Chang I-W, Smith BL et al (1998) Evaluating human breast ductal carcinomas with high-resolution magic-angle spinning proton magnetic resonance spectroscopy. J Magn Reson 135:194–202
11. Peeling J, Sutherland G (1992) High-resolution ^{1}H NMR spectroscopy studies of extracts of human cerebral neoplasm. Magn Reson Med 24:123–136
12. Beckonert O, Monnerjahn J, Bonk U et al (2003) Visualizing metabolic changes in breast-cancer tissue using 1H-NMR spectroscopy and self-organizing maps. NMR Biomed 16:1–11
13. Hagberg G (1998) From magnetic resonance spectroscopy to classification of tumors. A review of pattern recognition methods. NMR Biomed 11:148–156
14. Lindon JC, Holmes E, Nicholson JK (2001) Pattern recognition methods and applications in biomedical magnetic resonance. Prog Nucl Magn Reson Spectrosc 39:1–40
15. Martens H, Næs T (1991) Multivariate calibration. Wiley, New York
16. Fan TWM (1996) Metabolite profiling by one- and two-dimensional NMR analysis of complex mixtures. Prog Nucl Magn Reson Spectrosc 28:161–219
17. Garrod S, Humpfer E, Spraul M et al (1999) High-resolution magic angle spinning ^{1}H NMR spectroscopic studies on intact rat renal cortex and medulla. Magn Reson Med 41:1108–1118
18. Künnecke B, Delikatny EJ, Russell P et al (1994) Proton magnetic resonance and human cervical neoplasia. II. Ex vivo chemical-shift microimaging. J Magn Reson B 104:135–142
19. Semenza GL, Artemov D, Bedi A et al (2001) The metabolism of tumors: 70 years later. Novartis Foundation Symposium 240:251–264
20. Dang CV, Semenza GL (1999) Oncogenic alterations of metabolism. Trends Biochem Sci 24:68–72
21. Warburg O. (1930) The metabolism of tumors. Constable, London
22. Gribbestad IS, Singstad TE, Nilsen G et al (1998) In vivo ^{1}H MRS of normal breast and breast tumors using a dedicated double breast coil. J Magn Reson Imaging 8:1191–1197
23. Gribbestad IS, Petersen SB, Fjøsne H et al (1994) ^{1}H NMR Spectroscopic characterization of perchloric acid extracts from breast carcinomas and non-involved breast tissue. NMR Biomed 7:181–194

24. Gribbestad IS, Sitter B, Lundgren S et al (1999) Metabolite composition in breast tumors examined by proton nuclear magnetic resonance spectroscopy. Anticancer Res 19:1737–1746
25. Lehnhardt FG, Rohn G, Ernestus RI et al (2001) ^{1}H- and ^{31}P-MR spectroscopy of primary and recurrent human brain tumors in vitro: malignancy-characteristic profiles of water soluble and lipophilic spectral components. NMR Biomed 14:307–317
26. Walenta S, Wetterling M, Lehrke M et al (2000) High lactate levels predict likelihood of metastases, tumor recurrence, and restricted patient survival in human cervical cancers. Cancer Res 60:916–921
27. Louw L, Engelbrecht AM, Cloete F (1998) Comparison of the fatty acid compositions in intraepithelial and infiltrating lesions of the cervix: part I, total fatty acid profiles. Prostaglandins Leukot Essent Fatty Acids 59:247–251
28. Engelbrecht AM, Louw L, Cloete F (1998) Comparison of the fatty acid compositions in intraepithelial and infiltrating lesions of the cervix: part II, free fatty acid profiles. Prostaglandins Leukot Essent Fatty Acids 59:253–257
29. Farrant RD, Lindon JC, Nicholson JK (1994) Internal temperature calibration for ^{1}H NMR spectroscopy studies of blood plasma and other biofluid. NMR Biomed 7:243–247